

Grain Size – Properties Correlation in Polycrystalline Hydroxyapatite Bioceramic

S. Ramesh

Department of Mechanical Engineering

College of Engineering

Universiti Tenaga Nasional

Km-7, Jalan Kajang-Puchong, 43009 Kajang, Selangor, Malaysia.

Abstract : The effect of grain size on the sintered properties of commercially available hydroxyapatite (HA) was investigated. HA disc samples were prepared by uniaxial pressing at 30 MPa and followed by cold isostatic pressing the powder at 200 MPa. In order to fulfill the objectives of the present work, the samples were subsequently sintered in air at various temperatures ranging from 1200°C to 1450°C in order to vary the grain sizes of the ceramic. Characterisation was carried out where appropriate to determine the phases present, bulk density, Vickers microhardness and grain sizes. SEM analysis of the sintered microstructure revealed an exponential increase in grain size with increasing sintering temperature. It was found that the hardness and relative density of the material decreased as the grain size exceeded a certain lower and upper limit respectively.

Abstrak : Kajian saiz butir pada sifat HA komersial yang telah disinter diselidik. Sample ceper HA telah disediakan dengan menggunakan penekanan uniaksial pada 30 MPa dan ini dikuti dengan penekanan sejuk isostatik pada 200 MPa. Dalam memenuhi objektif kajian ini, sample telah disinter dalam udara pada pelbagai suhu yang menjulat dari 1200°C hingga 1450°C untuk mempelbagaikan saiz butir seramik. Penyifatan telah dijalankan dimana bersesuaian, untuk menentukan fasa yang timbul, kepadatan pukal, mikrokekerasan Vickers dan saiz butir. Analisa SEM mikrostruktur yang disinter mendedahkan bahawa terdapat pertambahan eksponen dalam saiz butir apabila suhu sinter dinaikkan. Kajian ini menunjukkan bahawa kekerasan dan kepadatan relatif bahan semakin berkurang apabila saiz butir melebihi had tinggi dan rendah masing-masing.

Received 12.4.01; accepted 11.9.01

Introduction

Bone is a composite material made up of 60 to 70% inorganic mineral crystals and 30 to 40% organic matrix consisting mostly of collagen protein fibers. The major mineral constituent of bone is hydroxylapatite (HA) or $\text{Ca}_{10}(\text{PO}_4)_6(\text{OH})_2$, in the form of tiny elongated crystals [1, 2]. These crystals are combined with the collagen fiber organic matrix of bone in a highly organized fashion and stiffen the bone structure analogous to the way that glass fibers stiffen softer plastics in the synthetic composite fiberglass.

Synthetically prepared hydroxylapatite ceramic has the same chemical composition as this major mineral constituent of bone. Corals create a calcium carbonate exoskeleton resembling human bone with an average pore size of 200 microns. The calcium carbonate skeleton can then be converted into HA through an exchange reaction of the carbonate for phosphate. The resultant material has a porous anatomy of bone with identical chemical composition.

HA implants are rapidly invaded by fibrovascular tissue and there is histologic evidence of direct osseous union between implant and bone which in turn encourages better fixation of implants [3]. In addition, HA is osteoconductive, in that it provides a matrix for deposition of new bone from adjacent living bone. It has excellent maintenance of contour and volume and HA implants do not elicit a foreign body or inflammatory response [4, 5].

As such, today, there is a wide use of HA as coating material on prosthetic metallic implant [6]. HA coated implants allow natural bone re-growth to occur until close contact has been achieved between natural bone and the HA coating hence results in excellent fixation of the prosthesis [7, 8].

However, as a ceramic material, hydroxyapatite is quite brittle; for example if the coating on the implant surface is too thick ($> 70 \mu\text{m}$), then failure of fixation between the bone and the prosthesis may occur through cracks which develop within the substance of the coating [9]. In addition to the low strength (i.e. $< 120 \text{ MPa}$) and low fracture toughness (i.e. $\sim 1 \text{ MPam}^{1/2}$) of the material, the use of HA solid or porous implant is limited to non-load bearing applications [10].

Efforts to improve the strength of HA have focused on the incorporation of foreign particles into the HA matrices to form composites that might induce energy dissipative mechanisms such as crack deflection, thus enhancing the mechanical properties [11]. This has shown to yield better strength, but is often associated with the formation of undesirable phases in the composite due to the higher sintering temperatures employed [12].

The present work focused on the effects of grain size on the sintered properties of HA ceramics made from a commercially available powder. In addition, preliminary investigation was carried out to study the decomposition of HA and subsequent effects on the relative density and hardness.

Methods and Materials

The starting HA was a commercially available powder (Merck 2196, Germany) having a Ca to P weight ratio of 2.14 or a molar ratio of 1.67 ± 0.02 . The morphology of the starting powder was examined using a Philips XL40 scanning electron microscope (SEM). The particle size distribution of the powder was obtained using a Coulter Laser Particle Size Analyser with a sensitivity of $0.4 \mu\text{m}$. Prior to this measurement, the powder was mixed in distilled water and treated in an ultrasonic bath for 10-15 minutes in order to break any agglomerates. The as received HA powder was uniaxial pressed at 40 MPa into pellets using a 20 mm cylindrical die and subsequently cold isostatically pressed (CIP) at 200 MPa. As expected, the CIP green pellets exhibited a linear shrinkage of 10%. The pellets were then sintered in air at various temperatures ranging from 1200°C to 1450°C at a furnace ramp rate of $2^\circ\text{C}/\text{min}$. and soaking time of 2 hours in order to vary the grain sizes.

Sintered pellets were ground and mirror polished to $1 \mu\text{m}$ surface finish using diamond paste. The bulk density of the samples was determined by Archimedes' method using distilled water. The relative density was obtained by assuming the theoretical density of hydroxyapatite as 3.156 g cm^{-3} .

The crystalline phases present in the samples were identified by using a Rigaku D-MAX X-ray diffractometer with Cu-K α radiation source at a scan speed of 0.5° per minute and a step scan of 0.02° . The different phases were identified with reference to standard JCPDS cards available in the system software. In addition, microstructural evolution under the various sintering temperatures was examined using scanning electron microscope. Prior to SEM analysis, the polished samples were etched with 0.5% HF to delineate the grain boundaries. The average grain size was determined from scanning electron micrographs using the line intercept analysis of Mendelson [13].

Hardness of the samples was measured using the Vickers indentation method. The indentation load was kept constant at 1.96 N (200 grams) and was applied for 10 seconds. Average hardness value was taken from at least five indents made for each sample and the maximum error obtained was found to be $< 5\%$.

Results and Discussion

Powder Morphology & Phase Stability

The average powder particle size was measured to be about $11 \mu\text{m}$ with a median of about $6 \mu\text{m}$. SEM micrograph of the powder, as shown in Fig. 1, shows that a wide range of particle size distribution exists. The larger particles ($\sim 10\text{-}15 \mu\text{m}$) typically observed in Fig. 1 are soft agglomerates which breaks easily during compaction.

The crystalline phases that were detected in the fired samples are presented in Table I. It was found that the HA phase was stable in samples sintered below 1400°C . Fig. 2 (a) shows the X-ray diffraction

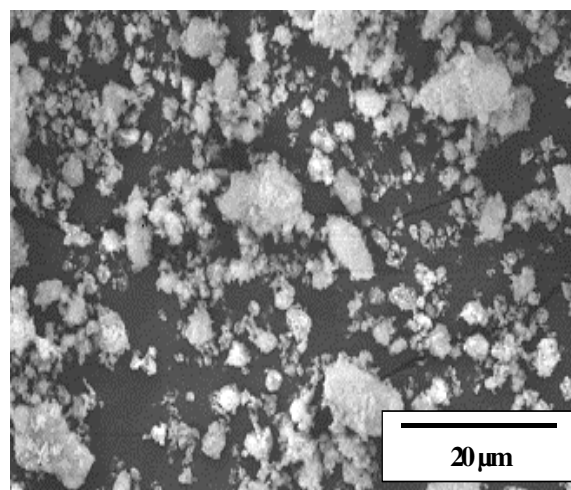


Fig. 1. Scanning electron micrograph of the commercial HA powder exhibiting the presence of soft agglomerates.

(XRD) pattern of a sample consisting of only the HA phase which is in agreement with the standard JCPDS file No. 9-432 for hydroxyapatite. Decomposition of the HA phase was observed with the presence of tricalcium phosphate (TCP) in samples sintered at 1400°C as shown in Fig. 2 (b). However, an increase in the sintering temperature above 1400°C produced detrimental results, which caused further decomposition of HA thus forming tetracalcium phosphate (TTCP) and calcium oxide (CaO), Fig. 2 (c).

Table I. Phases present in the samples sintered at various temperatures.

Sample	Sintering temperature ($^\circ\text{C}$)	Phases detected by XRD
HA-1	1200	HA
HA-2	1250	HA
HA-3	1300	HA
HA-4	1350	HA
HA-5	1400	HA, α -TCP
HA-6	1450	HA, α -TCP, β -TCP, TTCP, CaO

In general, the decomposition temperature (i.e. 1400°C) of HA observed in this work is considered higher than the usual temperature (i.e. 1300°C) reported by other workers. The difference in the results in the present work could be, in part, attributed to the relatively high humidity content present in the sintering atmosphere. It is believed that the high humidity content slows down decomposition

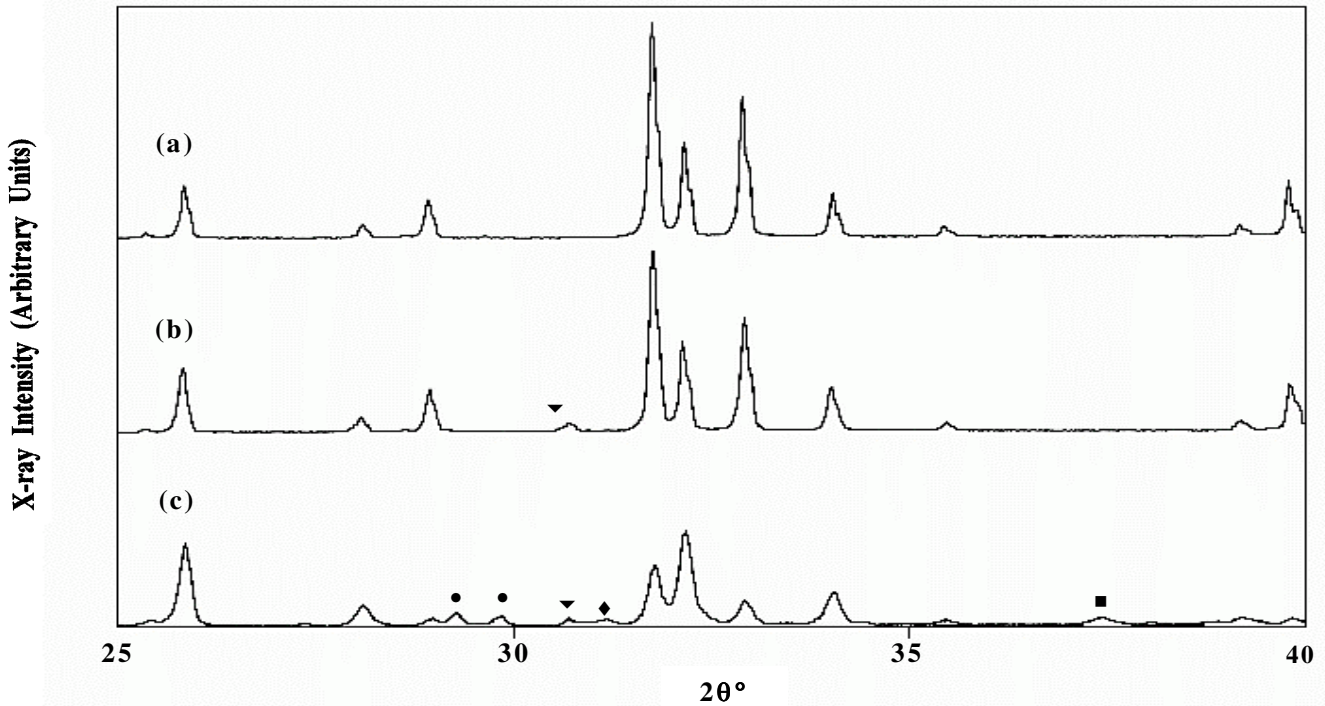


Fig. 2. X-ray diffraction patterns of HA sintered for 2 hours at (a) 1250°C, (b) 1400°C and (c) 1450°C. All the peaks in (a) correspond to the HA phase. (Key : • = TTCP ; ▼ = α -TCP ; ◆ = β -TCP and ■ = CaO).

rate by preventing dehydration of the OH group from the HA matrix. Similar observations were also encountered by Wang and Chaki [14].

Relative Density

The relative densities of the HA sintered at various temperatures are shown in Fig. 3. It was found that samples with an average grain size of $\sim 1.2 \mu\text{m}$ (i.e. sintered at 1200°C) exhibited the lowest relative density of 95.7% whereas the highest relative density of 99.8% was attained in samples that have larger average grain size of $\sim 12.3 \mu\text{m}$ (i.e. sintered at 1400°C). The low bulk density of the former was

attributed to the low densification temperature employed resulting in the presence of residue porosity located mainly at grain boundaries, as seen during the SEM investigation [15]. As the sintering temperature was increased beyond 1200°C, the samples exhibited densities $> 99\%$ with remnant porosity remaining in the structure. However, as the grain size exceeded $12.3 \mu\text{m}$ (i.e. sintering $> 1400^\circ\text{C}$) this was accompanied by a decline in the bulk density which could have been due to the presence of various other phases in the sample resulting from the decomposition of HA.

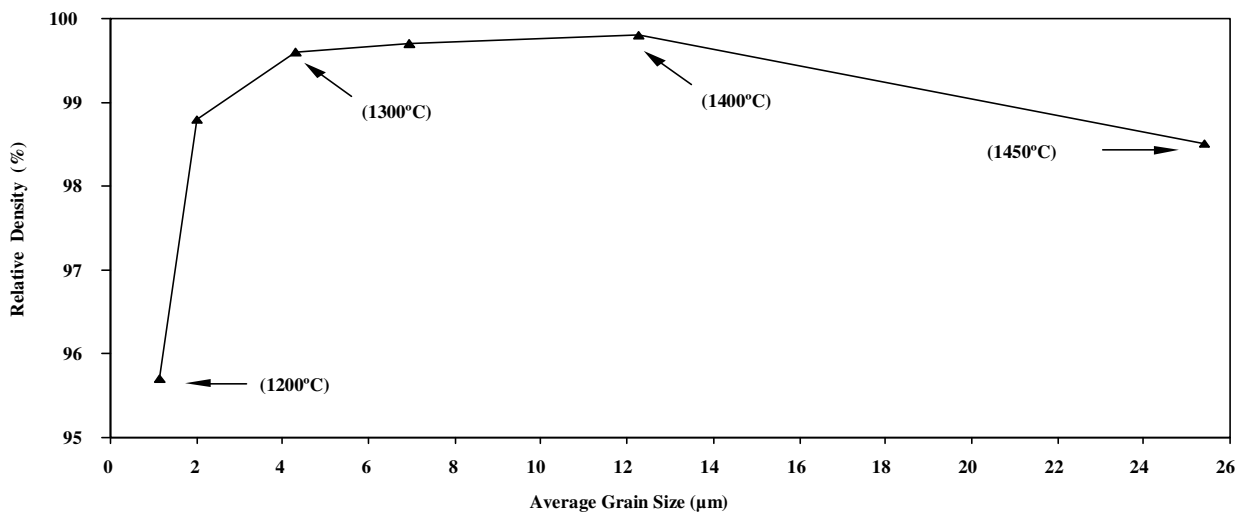


Fig. 3. The effect of grain size on the relative density of HA. The values in parentheses indicate the sintering temperature

Hardness

The change in Vickers hardness with grain sizes for samples sintered at various temperatures are presented in Fig. 4. It was found that samples with an average grain size of $\sim 2 \mu\text{m}$ (i.e. sintered at 1250°C) exhibited the highest hardness of $6.08 \pm 0.28 \text{ GPa}$. The low hardness obtained for samples sintered at 1200°C is in agreement with the low measured bulk density. In contrast, as the grain sizes increases beyond $2 \mu\text{m}$ resulting from sintering above 1250°C ,

the ceramic exhibited a gradual decrease in hardness even though they possessed relative high density values of more than 99% as clearly shown in Fig. 5. The fact that the sample with the highest relative density exhibited low hardness (Fig. 5), suggested that a grain size effect could be responsible for the decrease in the hardness of HA. However, further work on this phenomenon is still in progress and will be reported in subsequent paper.

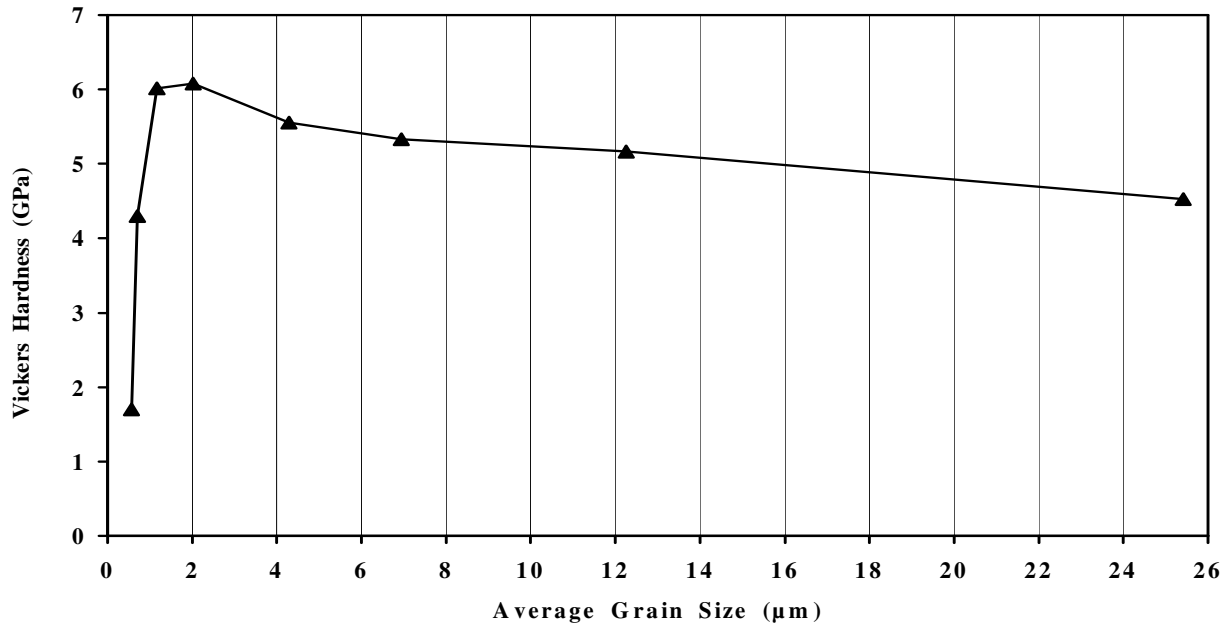


Fig. 4. The effect of grain size on the Vickers hardness of hydroxyapatite.

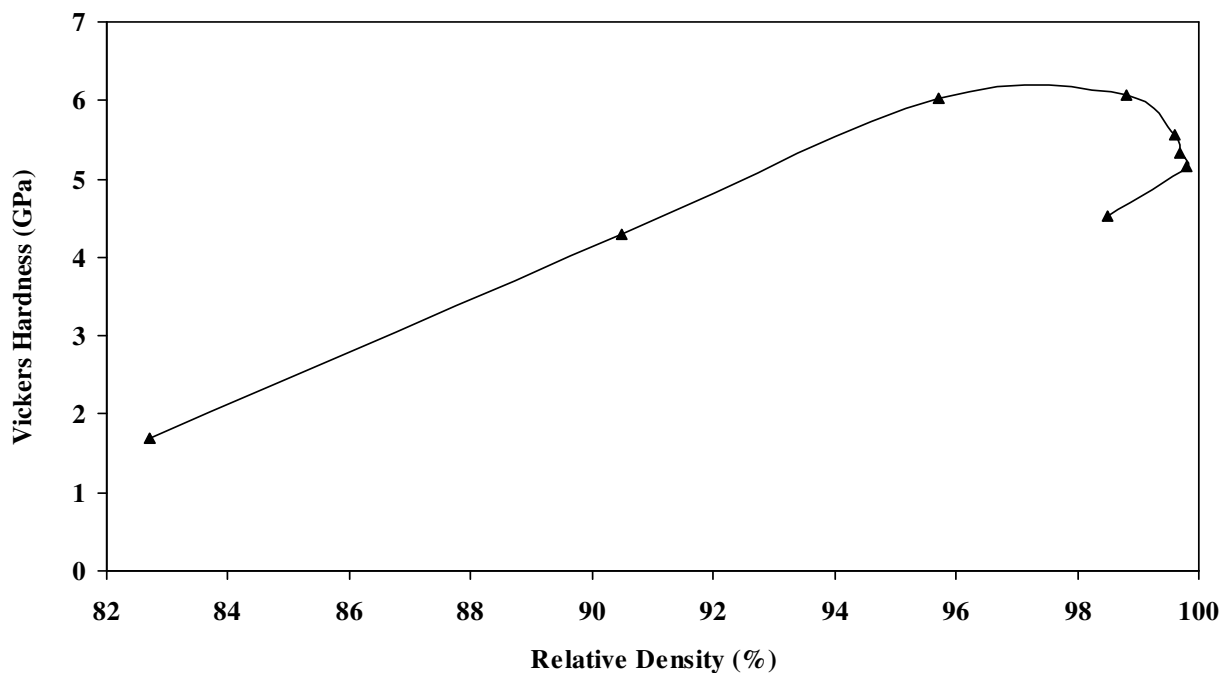


Fig. 5. The influence of relative density on the Vickers hardness of HA.

Microstructural Evolution

The microstructural evolution of HA sintered at 1200°C and 1400°C are shown in Fig. 6. The initial SEM investigation revealed that when sintered at low temperatures, the HA exhibited a uniform microstructure and distribution of equiaxed fine grains which indicated the high degree of homogeneity of the starting powder. However, as the sintering temperature was increased further, this was accompanied by grain coalescence with occasionally exaggerated grain growth being observed in HA sintered $\geq 1400^\circ\text{C}$ (see Fig. 6b). The dramatic change in the average grain size with sintering temperature is depicted in Fig. 7. It was found that as the sintering temperature was increased from 1200°C to 1450°C, the average grain size increased exponentially from 1.16 μm to 25.41 μm respectively. However at this stage, this grain growth phenomenon is still unclear.

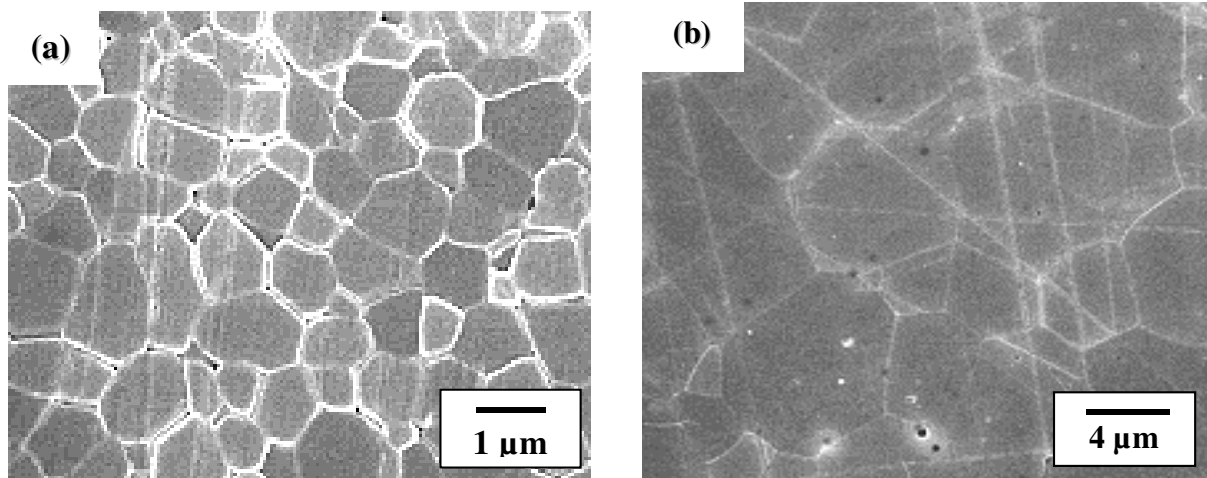


Fig. 6. SEM micrographs of HA showing an equiaxed-grained structure when sintered at (a) 1200°C and (b) 1400°C. Exaggerated grain growth is evident in (b).

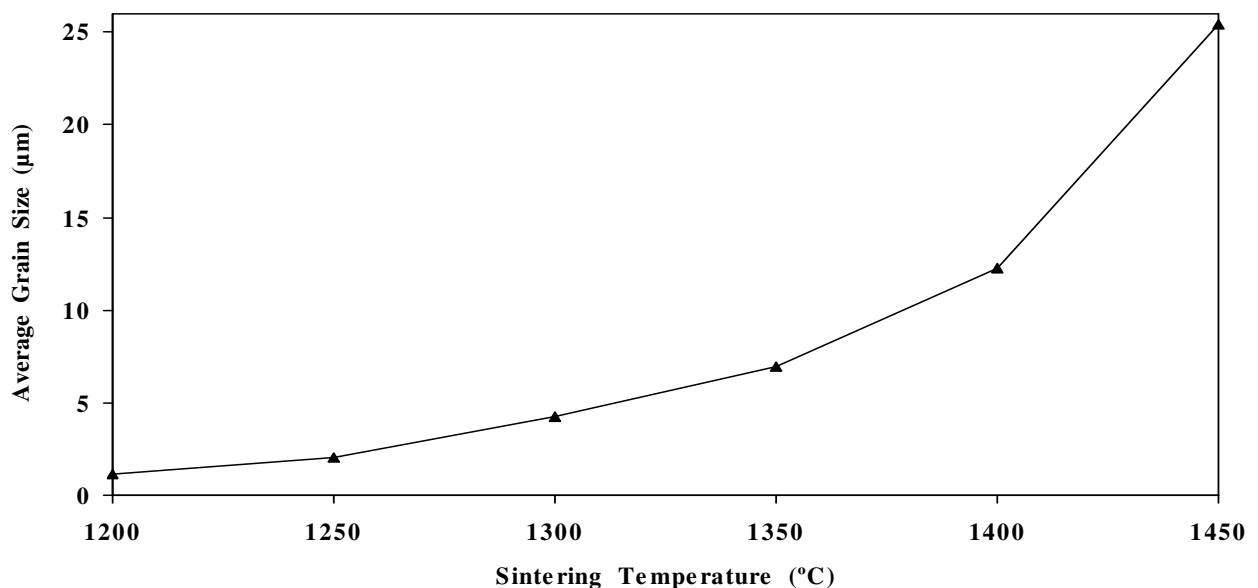


Fig. 7. The effect of sintering temperature on the average grain size of HA.

Conclusions

1. In the present study, the results showed that microstructural parameters such as the grain size have a profound effect that influence the properties of a stoichiometric commercial HA.
2. The study revealed that HA phase was stable when sintered below 1400°C for 2 hours. However, sintering $\geq 1400^\circ\text{C}$ resulted in the decomposition of HA to form TCP, TTCP and CaO.
3. The average HA grain size was found to increase exponentially with increasing sintering temperature. This in turn was found to have a positive and negative effect on the density of the material. It was found that as the grain size started to increase above a certain upper grain size limit, e.g. 12.3 μm , the relative density started to decrease below 99%.

4. On the other hand, the hardness started to decrease above a certain lower grain size limit, e.g. $\sim 2 \mu\text{m}$. In addition, it was also revealed that the hardness of the material was not solely dependent on the relative density.

Acknowledgements

The author gratefully acknowledges the Department of Mechanical Engineering, UNITEN for the continuing support and the Ceramics Technology Centre, SIRIM Berhad for providing the testing facilities in this work.

References

- Jarcho, M., Bolen, C. H., Thomas, M. B., Bobick, J., Kay, J. F. and Doremus, R. H. (1976) *J. Mater. Sci.*, **11**, 2027.
- Akoi, H., Kato, K., Ogiso, M. and Tabata, T. (1977) *J. Dental Outlook*, **49**, 567.
- Gregoire, M., Orly, I. And Menateau, J. (1990) *J. Biomed. Mater. Res.*, **24**, 165-177.
- Jarcho, M. (1981) *Clin. Orthop. Rel. Res.*, **157**, 259.
- Oonishi, H. (1991), *Biomaterials*, **12**, 171.
- Watson, C. J., Tinsley, D., Ogden, A. R., Russell, J. L., Mulay, S. and Davison, E. M. (1999) *British Dental Journal*, **187** (2), 90-94.
- Capello, W. N., D'Antonio, J. A., Feinberg, J. R. and Manley, M. (1997) *The Journal of Bone and Joint Surgery*, **79-A** (7), 1023-1029.
- Brossa, F., Cigada, A. and Chiesa, R. (1993) *Biomed. Mater. Eng.*, **3** (3), 127-136.
- Kitsugi, T., Nakamura, T., Oka, M., Senaha, Y., Goto, T. and Shibuya, T. (1996) *J. Biomed. Mater. Res.*, **30**, 261-269.
- Akao, M., Aoki, H. and Kato, K. (1981) *J. Mater. Sci.*, **16**, 809.
- Lange, F. F. (1982) *J. Mater. Sci.*, **17**, 225.
- Ramesh, S. and Muralithran, G. (2001) *Biomedical Engineering: Applications, Basis & Communications*, **13** (2), 66-71.
- Mendelson, M. I. (1969) *J. Am. Ceram. Soc.*, **52**, 443.
- Wang, P. E. and Chaki, T. K. (1993) *J. Mater. Sci. Mater. in Med.*, **4**, 150.
- Muralithran, G. and Ramesh, S. (2000) *Ceramics International*, **26**, 221-23

